Rapid Deceleration-Driven Wetting Transition during Pendant Drop Deposition on Superhydrophobic Surfaces

Hyuk-Min Kwon, Adam T. Paxson, Kripa K. Varanasi, and Neelesh A. Patankar

Phys. Rev. Lett. **106**, 036102 — Published 20 January 2011

DOI: 10.1103/PhysRevLett.106.036102

Rapid deceleration driven wetting transition during pendant drop deposition on superhydrophobic surfaces

Hyuk-Min Kwon,[1] Adam T. Paxson,[1] Kripa K. Varanasi,[1,*] Neelesh A. Patankar[2,*]

[1]Department of Mechanical Engineering, Massachusetts Institute of Technology
77 Massachusetts Avenue, Cambridge, MA 02139-4307

[2]Department of Mechanical Engineering, Northwestern University
2145 Sheridan Road, B224, Evanston, IL 60208–3111

Abstract

A hitherto unknown mechanism for wetting transition is reported. When a pendant drop settles upon deposition, there is a virtual "collision" where its center of gravity undergoes rapid deceleration. This induces a high water hammer-type pressure that causes wetting transition. A new phase diagram shows that both large and small droplets can transition to wetted states due to the new deceleration driven and the previously known Laplace mechanisms, respectively. It is explained for the first time how the attainment of a non-wetted Cassie-Baxter state is more restrictive than previously known.

[*] Corresponding authors: varanasi@mit.edu (experimental/analytical); n-patankar@northwestern.edu (analytical).

Textured surfaces have gained widespread attention due to their utility in a variety of applications such as self–cleaning surfaces, low drag (high slip) materials, substrates for efficient dropwise condensation heat transfer, among others.[1-4] The performance in many applications relies greatly on the wetting state of liquid droplets on rough hydrophobic surfaces. In one of the states, droplets reside on top of roughness features, i.e. in a Cassie-Baxter (CB) state.[3] Droplets that impale the roughness grooves, i.e., in a Wenzel state,[3] represent another commonly observed scenario. Recent experimental work has successfully revealed pressure–induced transition from the CB to the Wenzel state on rough hydrophobic substrates with pillar geometries.[5-14] There are two primary mechanisms by which transition can be induced by high pressure of the liquid: de–pinning and sag mechanisms.[6, 7, 10, 14] A liquid–air interface hangs between pillars in the CB state. The interface is curved due to the pressure difference across it.[7, 10, 14] If the hanging interface is such that it cannot remain pinned at the pillar tops, then it proceeds downward into the roughness grooves and fully wets the surface. Even when a liquid–air interface can remain pinned at the pillar tops, transition to the Wenzel state is possible if the sag in the curved liquid–air interface is such that it touches the bottom of the roughness groove.[7, 10]

For a droplet to remain in the CB state, the transition–inducing wetting pressures P_{wet} must be less than the anti–wetting pressure $P_{antiwet}$ which is the capillary pressure P_C in the case of a textured surface.[5-13] In the case of a Laplace pressure–induced transition, a *smaller* droplet will more readily transition to a Wenzel state. Another mechanism of transition, driven by gravity, was implicated by Yoshimitsu *et al.*[15] They found that *larger* droplets, above a critical size, transitioned to the Wenzel state. This result is opposite of the Laplace pressure–induced transition. This is surprising because the water droplets used in their experiments[15] were 1–12 mg, where gravity is not expected to play a dominant role during deposition. Usually, gravity is expected to be comparable to or larger than the surface tension forces for water droplets 82 mg or larger.[16] It has remained unclear if these data are repeatable, or, if repeatable, the details of the transition process are unclear. Our goal is to revisit this long standing and unresolved claim about gravity–based transition at small scales.[15]

Careful experiments are reported here with two different methods of depositinga droplet on the substrate. It is found that if deposited quasi–statically, which will be elaborated in this paper, the CB droplet *does not* undergo gravity–driven transition to a Wenzel state. However, when a

pendant drop is deposited, transition is induced – the cause for which will be explained based on a new decelration-driven mechanism. This mechanism has broader implications to droplet impact[6], wetting on vibrating surfaces[8], and wetting in inkjet printing.[17]

The wetting experiments reported here were conducted on superhydrophobic surfaces consisting of arrays of 10 μm square posts, shown in Fig. 1(a). The Si micropost arrays were fabricated via standard photolithography processes and modified with a thin coating of fluorosilane (tridecafluoro-1,1,2,2 tetrahydrooctyl-trichlorosilane, Sigma Aldrich) by vapor phase deposition. The advancing contact angle of water on smooth fluorinated silicon was measured using a goniometer to be $120° \pm 3°$. The array of square posts produced superhydrophobic surfaces whose capillary pressure P_C is given by[18, 19]

$$P_C = \frac{\sigma}{a}\left[\frac{-4\cos\theta_a}{(1+b/a)^2 - 1}\right], \qquad (1)$$

where σ is the surface tension of water, θ_a is the advancing contact angle on a smooth surface, a is the post width, and b is the spacing between posts. The wetting experiments were performed with various droplet volumes using two deposition methods. The wetting transition was detected by a dramatic decrease in contact angle and increase in droplet adhesion. Droplet volume was controlled with an automatic dispensing system having a volume step resolution of 0.02 μL. In the first method, to approximate a quasi–static deposition, droplets were deposited onto surfaces with post spacings ranging from 40 to 75 μm using a 30–gauge stainless steel needle so as to minimize the adhesion forces of the needle. After forming a stable CB sessile droplet on the textured substrate, its volume was increased at a rate of 0.2 μL per second. The needle was not detached from the droplet. As the volume of these CB droplets increased, no transition was observed even as the droplet volumes surpassed 500 μL (500 mg). The droplet seen in Fig. 1(b) & (c) provides unambiguous evidence that a gravity–based transition is not observed even for droplets much larger than the critical mass of 82 mg where gravitational and surface tension forces are of the same order for water. These results are contrary to the observations of Yoshimitsu *et al.*[15]

The second method is based on "gentle" deposition of a droplet on the surface. To obtain a sessile droplet, it is necessary to detach a pendant droplet from the dispensing needle. The

droplet deforms due to the adhesion forces of the needle, which scale with needle diameter. Different needle sizes were selected so that pendant droplets would detach at volumes ranging from 7 μL to 90 μL. After forming a pendant droplet that is slightly smaller than the detachment volume, the droplet was lowered as close to the substrate as possible to be detached by further addition of volume, which results in necking at the top of the droplet and subsequent detachment onto the substrate.[20] Substrates with different post spacings (edge–to–edge), ranging from 40μm to 100μm, were used in the experiments.

As shown in Fig 2, it is apparent that large droplets did not transition on 40 μm spaced posts; even droplets with volumes of 75 μL remained in the CB state. Only when a droplet was evaporated below its critical Laplace transition volume (0.03 μL) did we observe a Wenzel droplet on the dense 40 μm spaced substrate. The medium (60 to 87.5 μm) spaced substrates exhibited a volume–dependent wetting behavior. For example, on the 75μm spaced substrate shown in Fig 2, transition was observed for 1 μL droplets, no transition for 11 μL or 55 μL droplets, but surprisingly, droplets with a volume of 75 μL transitioned to the Wenzel state. On the sparse 100 μm spaced substrate, we observed that all droplet sizes, ranging from 7 μL to 75 μL, underwent transition. Although the pendant droplets remained in the CB state when brought into contact with the 100 μm spaced sample, they were observed to transition to the Wenzel state upon detachment from the needle. These experimental observations show for the first time that the CB–to–Wenzel transition can occur not only for small droplets (due to the well understood Laplace mechanism) but also for large droplets.

To further understand the transition of larger droplets, high–speed images of wetting interactions during "gentle" deposition of large droplets were recorded at 8500 fps. The image sequence for the 75 μm spaced substrate is shown in Fig. 3 and the corresponding movie is provided in Supplementary Material. It is seen that initially, as the droplet settles on the substrate, there are surface perturbations and shape changes. A dominant feature that is observed is that the center of gravity (CG) of the droplet is lowered by a length scale $\Delta \sim 1\,\text{mm}$ on a time scale $t_{fall} \sim 10\,\text{ms}$ that corresponds to the free fall time scale (i.e., $\Delta \sim g t_{fall}^2$). This motion of the CG gives rise to a velocity $V_{fall} = \sqrt{2g\Delta}$ of the CG (see Supplementary Material).

If it is assumed that the pressure scales as the convective term in the fluid equations, then the corresponding steady Bernoulli–type dynamic wetting pressure $P_D = \rho V_{fall}^2 / 2$. This pressure is calculated here to be on the order of 10 Pa. The anti–wetting capillary pressure P_C, calculated for 75 μm spacing using Eq. (1), is 202 Pa and far exceeds the steady Bernoulli–type dynamic wetting pressure of 10 Pa calculated above. Therefore, it cannot explain the transition of the droplet to the Wenzel state. The high–speed images in Fig. 3 show that the CG stops moving down, representing a virtual "collision" with the substrate, in a very short time scale that is less than the millisecond scale time resolution of the high speed camera. Transition to the Wenzel state occurs during this time, and is followed by capillary waves. We propose that during this rapid deceleration, the pressure must scale predominantly with the time derivative inertia term in the fluid equations (unsteady Bernoulli equation). Rapid deceleration can produce a large water–hammer–type pressure[6] that is given as $P_{WH} = k\rho V_{fall} C$, where k is a constant depending on the type of collision, shape, and velocity of the droplet;[21] and C is the speed of sound. For the current scenario with low velocity and large droplet size, $k = 0.001$ (see Supplementary Material). This implies $P_{WH} = 2000$ Pa, which is significantly larger than the anti–wetting capillary pressure to cause transition. Thus, energy can be channeled by rapid deceleration into a large water hammer–type pressure that can result in transition to the Wenzel state.

Next, we estimate the critical size of the droplets that can undergo CB–to–Wenzel transition via the deceleration mechanism. The displacement Δ can be estimated by considering the reduction in potential energy and the eventual gain in surface energy[22] as $\Delta \sim \rho g R^3 / \sigma$, where R is the radius of the droplet. As the volume of the droplet increases, so do Δ and V_{fall}, and, ultimately, the water hammer pressure. The capillary pressure P_C given in Eq. (1) can be generalized to arrays of posts with other prismatic cross–sections in terms of the solid–liquid contact perimeter P and the liquid–vapor interfacial area A projected onto a horizontal surface in one unit cell. It is given by **(**see Supplementary Material**)**

$$P_C = -\sigma P \cos\theta_a / A = \sigma / \ell_r , \qquad (2)$$

where ℓ_r defined in Eq. (2) is the length scale associated with the average radius of curvature of the liquid meniscus required to impale the roughness. The critical droplet radius R_{WH}^* for

transition can be obtained by equating the deceleration–based water hammer pressure P_{WH} to the capillary pressure P_C of the surface and is given by

$$\frac{R^*_{WH}}{\ell_r} = \left(\frac{\ell_\sigma}{\ell_C}\right)^{1/3}\left(\frac{\ell_\sigma}{\ell_r}\right)^{5/3}, \tag{3}$$

where $\ell_\sigma = \sqrt{\sigma/\rho g}$ is the capillary length based on the balance between the gravitational and surface energies. $\ell_C = 2k^2C^2/g$ is a length scale based on the balance between sound wave and gravitational energies. Similar expressions for critical droplet radii R^*_D, R^*_L based on the dynamic and Laplace pressures, respectively, are

$$\frac{R^*_D}{\ell_r} = \left(\frac{\ell_\sigma}{\ell_r}\right)^{4/3};\ \frac{R^*_L}{\ell_r} = 2. \tag{4}$$

According to the above mechanisms, transition will occur if $R > R^*_{WH}$ or R^*_D and if $R < R^*_L$. It is noted that the Laplace mechanism based condition for R^*_L is independent of the capillary length scale ℓ_σ, i.e., gravity does not play a role. This is as expected because the droplets are assumed to be smaller than the capillary length scale.[10] For square posts, it follows from Eq. (1) that $\ell_r = 2b(1+b/2a)/(-4\cos\theta_a)$. Thus, when b/a is small, $\ell_r \sim b/(-2\cos\theta_a)$, which implies that $R^*_L \sim b/(-\cos\theta_a)$. This is same as the scaling for Laplace pressure–based transition according to the de–pinning mechanism.[18] When b/a is large, $\ell_r \sim b^2/(-4a\cos\theta_a)$, which implies that $R^*_L \sim b^2/(-2a\cos\theta_a) \sim b^2/a$ (the last reduction in scaling is an equality when $\theta_a = 120^0$ as in our case). This is same as the scaling for transition according to the sag mechanism[7, 10] when the post height $H \sim a$; in our case $H = a$. Thus, in our case, the condition in Eq. (4) captures both the de–pinning and sag based transitions in their respective limits (see Supplementary Material). Eqs. (3) and (4) show that the capillary length scale becomes relevant in the case of water hammer–based or dynamic pressure–based mechanisms. Fig. 4 shows that the data are explained by the water hammer–based mechanism of transition.

In Fig. 4, we plot the critical radius of droplets as a function of the parameter $\chi \equiv \ell_r/\ell_\sigma$ and find good agreement with the experimental data presented in this paper. The region between the

Laplace and water hammer curves represents the CB regime while regions outside represents the Wenzel regime. Furthermore, it is interesting to note that the water hammer–based critical radius R^*_{WH} and Laplace–based critical radius R^*_L intersect when

$$\chi_{crit} = \left(\frac{\ell_r}{\ell_\sigma}\right)_{crit} = \left(\frac{\ell_\sigma}{8\ell_C}\right)^{1/5}. \quad (5)$$

Hence hydrophobic textures with $\chi \geq \chi_{crit}$ will always result in Wenzel wetting (such as the 100 μm spaced substrates in our experiments). Thus, it is seen that, both, large and small droplets transition to Wenzel states due to the deceleration and Laplace mechanisms, respectively. This results in a new regime of transition and a new phase diagram of droplet sizes in CB and Wenzel states.

In summary, we show that large droplets can undergo CB–to–Wenzel transition due to a rapid deceleration-induced water hammer–type mechanism during deposition. It can be argued that the source of energy for this transition could be the surface energy in the initially distorted droplet shape or the gravitational energy. We propose that the latter is plausible (see Supplementary Material). It is seen that as droplets settle on a substrate, even during "gentle" deposition, the center of gravity (CG) is lowered on the time scale of free fall. Then, the CG stops moving down, representing virtual "collision" with the substrate on a very short time scale. This rapid deceleration produces a water hammer-type pressure that scales with the unsteady inertia term and causes a wetting transition. A new phase diagram is presented, as shown in Fig. 4, where both small and large droplets can transition based on Laplace and water hammer mechanisms, respectively. This insight is novel and shows that the attainment of a CB state, in the scenarios considered in this paper, is more restrictive than previously known.

Acknowledgements KKV acknowledges support from MIT Energy Initiative and NSF CAREER Award. H-MK and ATP acknowledge support from Dupont-MIT Alliance and MIT Energy Initiative, respectively, for their graduate fellowships. NAP acknowledges support from the Initiative for Sustainability and Energy at Northwestern. We thank MIT's Edgerton Center and Dr. J. Bales for lending us their high-speed video equipments.

Figures

Figure 1

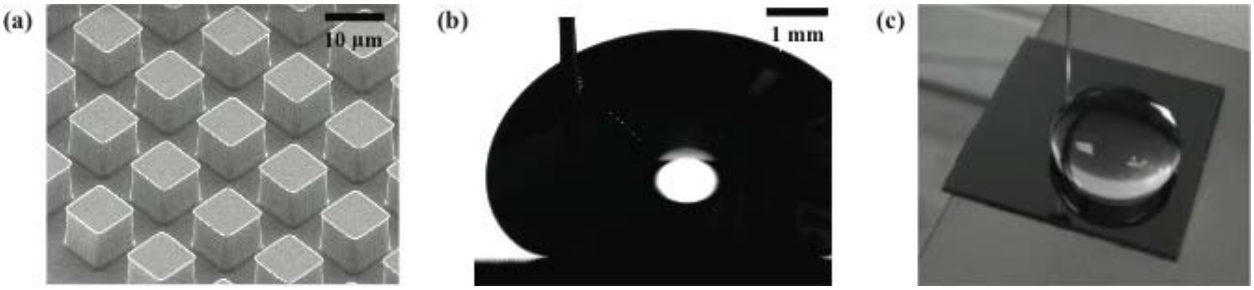

FIG. 1. (a) SEM (scanning electron microscope) image of 10μm tall 10 μm ×10 μm post structured hydrophobic surface. (b) A 150 μL CB droplet on a 75 μm spacing substrate and (c) a 500μL CB droplet on a 40 μm spacing substrate, as quasi-statically increased from a 5μL CB droplet. The edge of square substrate is 2 cm.

Figure 2

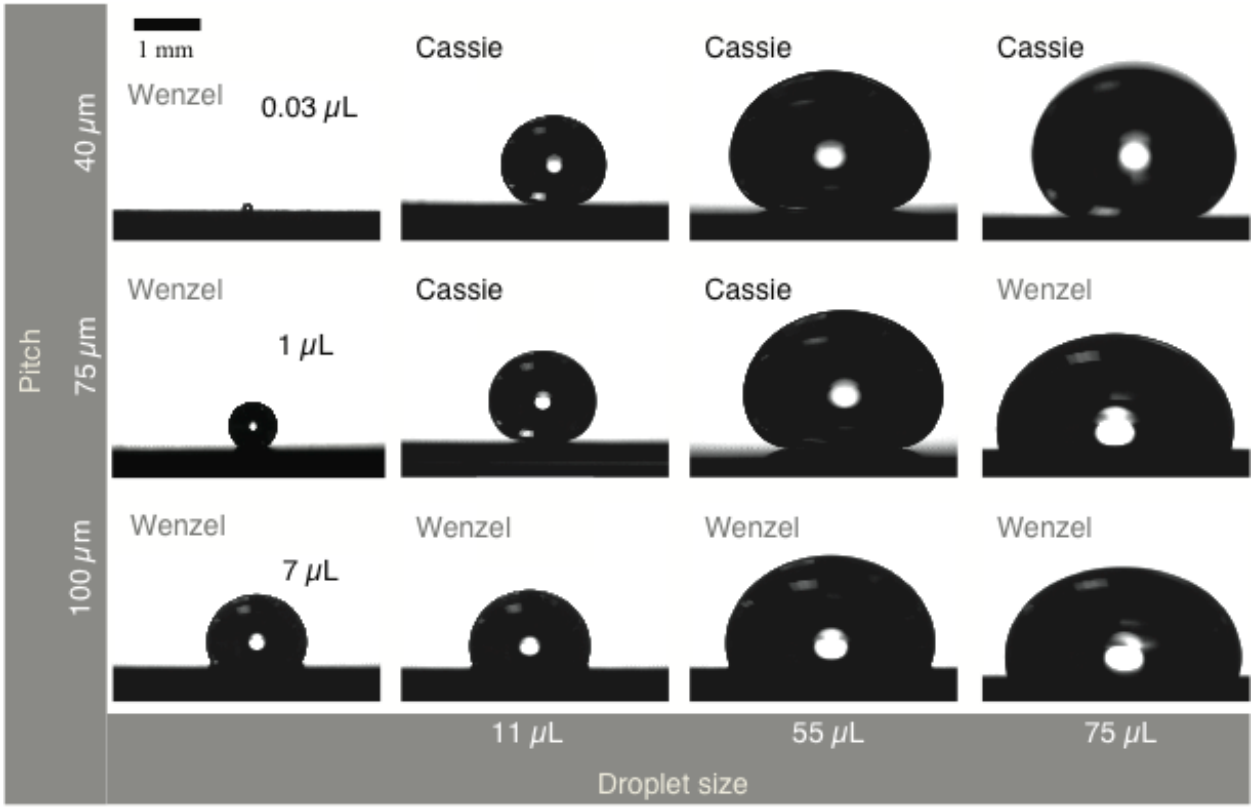

FIG. 2. Stable droplets with volumes from 0.03 μL to 75 μL "gently" deposited on textured hydrophobic surfaces with 10μm × 10μm × 10μm posts and varying pitch. Laplace pressure appears to cause transition of 0.03 μL and 1 μL droplets on 40 μm and 75 μm spaced samples, respectively.

Figure 3

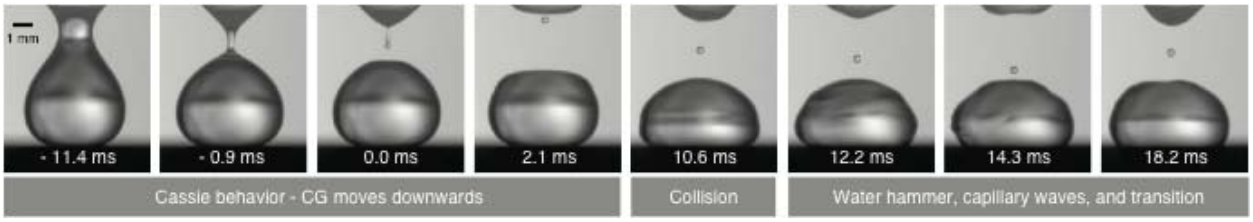

FIG. 3. High-speed image sequence of 75 μL droplet detachment and wetting transition on the 75 μm pitch textured substrate during a "gentle" droplet deposition. The transition event occurs between 10.6 ms and 12.2 ms. The time scale of CG motion corresponds to the free fall time scale followed by capillary waves and transition.

Figure 4

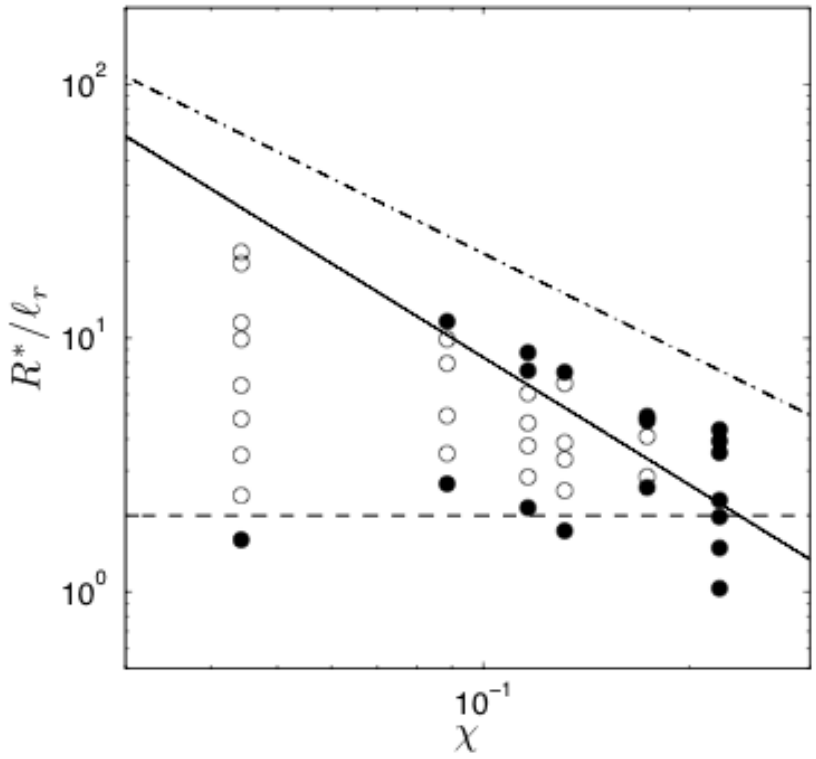

FIG 4. Size-dependent phase diagram of droplets in CB and Wenzel states on textured hydrophobic surfaces. Predictions for normalized critical radius R^*/ℓ_r, of water droplets that undergo CB-to-Wenzel transition as a function of the surface parameter $\chi = \ell_r/\ell_\sigma$ based on different wetting pressures: water hammer pressure (solid), Laplace pressure (dashed), and dynamic pressure (dash-dot). The region between the Laplace and water hammer curves represents CB regime while other regions represent the Wenzel regime. The experimental data are plotted as circles and consist of normalized droplet radii that are in CB (open circles) and Wenzel (filled circles) states.

References

1. C. Dietz, K. Rykaczewski, A. G. Fedorov and Y. Joshi, Applied Physics Letters **97** (3), - (2010).
2. N. A. Patankar, Soft Matter **6** (8), 1613-1620 (2010).
3. D. Quere, Annual Review of Materials Research **38**, 71-99 (2008).
4. K. K. Varanasi, M. Hsu, N. Bhate, W. S. Yang and T. Deng, Applied Physics Letters **95** (9), 094101 (2009).
5. D. Bartolo, F. Bouamrirene, E. Verneuil, A. Buguin, P. Silberzan and S. Moulinet, Europhysics Letters **74** (2), 299-305 (2006).
6. T. Deng, K. K. Varanasi, M. Hsu, N. Bhate, C. Keimel, J. Stein and M. Blohm, Applied Physics Letters **94** (13), Artn 133109 (2009).
7. Y. C. Jung and B. Bhushan, Scripta Materialia **57** (12), 1057-1060 (2007).
8. Y. C. Jung and B. Bhushan, Langmuir **25** (16), 9208-9218 (2009).
9. M. Reyssat, A. Pepin, F. Marty, Y. Chen and D. Quere, Europhysics Letters **74** (2), 306-312 (2006).
10. M. Reyssat, J. M. Yeomans and D. Quere, EPL **81** (2), 26006 (2008).
11. P. C. Tsai, R. G. H. Lammertink, M. Wessling and D. Lohse, Physical Review Letters **104** (11), - (2010).
12. A. Tuteja, W. Choi, J. M. Mabry, G. H. McKinley and R. E. Cohen, Proceedings of the National Academy of Sciences of the United States of America **105** (47), 18200-18205 (2008).
13. A. Tuteja, W. J. Choi, G. H. McKinley, R. E. Cohen and M. F. Rubner, Mrs Bulletin **33** (8), 752-758 (2008).
14. H. Kusumaatmaja, M. L. Blow, A. Dupuis and J. M. Yeomans, Epl **81** (3), Artn 36003 (2008).
15. Z. Yoshimitsu, A. Nakajima, T. Watanabe and K. Hashimoto, Langmuir **18** (15), 5818-5822 (2002).
16. N. A. Patankar, Langmuir **20** (17), 7097-7102 (2004).
17. J. U. Park, M. Hardy, S. J. Kang, K. Barton, K. Adair, D. K. Mukhopadhyay, C. Y. Lee, M. S. Strano, A. G. Alleyne, J. G. Georgiadis, P. M. Ferreira and J. A. Rogers, Nature Materials **6** (10), 782-789 (2007).
18. N. A. Patankar, Langmuir **26** (11), 8941-8945 (2010).
19. K. K. Varanasi, T. Deng, M. F. Hsu and N. Bhate, Proceedings of the Asme International Mechanical Engineering Congress and Exposition, Vol 13, Pts a and B, 637-645 (2008).
20. J. C. Bird, S. Mandre and H. A. Stone, Physical Review Letters **100** (23), - (2008).
21. O. G. Engel, Journal of Research of the National Bureau of Standards **54** (5), 281-298 (1955).
22. L. Mahadevan and Y. Pomeau, Physics of Fluids **11** (9), 2449-2453 (1999).